Available online at www.sciencedirect.com
ScienceDirect
Journal of Computational Physics 227 (2008) 2073–2082
JOURNAL OF COMPUTATIONAL PHYSICS
www.elsevier.com/locate/jcp

A new fourth-order Fourier–Bessel split-step method for the extended nonlinear Schrödinger equation

Patrick L. Nash *

Department of Physics and Astronomy, The University of Texas at San Antonio, San Antonio, TX 78249-0697, United States

Received 22 June 2007; received in revised form 27 September 2007; accepted 5 October 2007
Available online 26 October 2007

Abstract

Fourier split-step techniques are often used to compute soliton-like numerical solutions of the nonlinear Schrödinger equation. Here, a new fourth-order implementation of the Fourier split-step algorithm is described for problems possessing azimuthal symmetry in 3 + 1-dimensions. This implementation is based, in part, on a finite difference approximation $\triangle_{\perp}^{\mathrm{FDA}}$ of $\frac{1}{r}\frac{\partial}{\partial r}r\frac{\partial}{\partial r}$ that possesses an associated exact unitary representation of $e^{\frac{i}{4}\lambda\triangle_{\perp}^{\mathrm{FDA}}}$. The matrix elements of this unitary matrix are given by special functions known as the *associated Bessel functions*. Hence the attribute *Fourier–Bessel* for the method. The Fourier–Bessel algorithm is shown to be unitary and unconditionally stable.

The Fourier–Bessel algorithm is employed to simulate the propagation of a periodic series of short laser pulses through a nonlinear medium. This numerical simulation calculates waveform intensity profiles in a sequence of planes that are transverse to the general propagation direction, and labeled by the cylindrical coordinate z. These profiles exhibit a series of isolated pulses that are offset from the time origin by characteristic times, and provide evidence for a physical effect that may be loosely termed *normal mode condensation*. Normal mode condensation is consistent with experimentally observed pulse filamentation into a packet of short bursts, which may occur as a result of short, intense irradiation of a medium.

PACS: 02.30.Mv; 02.70.Bf; 02.30.Uu; 02.60.Cb; 02.30.Jr; 02.30.Gp

Keywords: Nonlinear Schrödinger equation; Split-step method; Normal mode condensation; Discrete Fourier; Associated Bessel

1. Introduction

The study of the nonlinear Schrödinger equation (NLSE) has been the focus of intense research for well over 30 years. [1–11]. Fourier split-step methods are regularly employed to calculate soliton-like numerical solutions of specific instances of the nonlinear Schrödinger class of equations, and have played a vital role in the study [1–6]. Nonlinear equations of the Schrödinger class govern the effective system dynamics in many diverse fields of physics. For example, the properties of a Bose–Einstein condensate [13–18] in a rotational

* Tel.: +1 210 458 5451.
E-mail address: Patrick.Nash@utsa.edu

0021-9991/$ - see front matter
doi:10.1016/j.jcp.2007.10.012

frame are modeled in Mean Field Theory at temperatures T much smaller than the critical condensation temperature T_c, by the well-known time-dependent Gross-Pitaevskii equation (GPE) with an angular momentum rotation term [13,15,17]:

$$-\frac{\hbar}{i}\frac{\partial\psi(\mathbf{r},t)}{\partial t}=\left(-\frac{\hbar^2}{2m}\nabla^2+V(\mathbf{r})+NU_0|\psi|^2-\Omega L_z\right)\psi(\mathbf{r},t),\quad t\geqslant 0, \tag{1}$$

where $\mathbf{r}=(x,y,z)^{\mathrm{T}}\in\mathbb{R}^3$, $\psi(\mathbf{r},t)$ is the complex-valued macroscopic wave function, m is an effective mass, N is the number of atoms in the condensate, Ω is the angular velocity of the rotating laser beam, $V(\mathbf{r})=\frac{m}{2}(\omega_x^2x^2+\omega_y^2y^2+\omega_z^2z^2)$, ω_x, ω_y and ω_z are the trap frequencies active along their respective coordinate axes, $U_0=\frac{4\pi\hbar^2a_s}{m}$ describes the interaction between atoms in the condensate with a_s the s-wave scattering length, and L_z is the z-component of the angular momentum.

Another important example is the extended nonlinear Schrödinger equation (ENLSE), which appears in the standard system of coupled equations for periodic femtosecond laser pulse propagation in a medium such as Argon or air [7–12]. When one writes the electric field $\overrightarrow{E}(r,z,t)$ in terms of a plane wave times a slowly varying complex envelope function $\overrightarrow{\mathcal{E}}(r,z,t)$ according to

$$\overrightarrow{E}(r,z,t)=\sqrt{\frac{\omega_0\mu_0}{2k_z}}\overrightarrow{\mathcal{E}}(r,z,t)\mathrm{e}^{\mathrm{i}(k_zz-\omega_0t)}+\text{c.c.} \tag{2}$$

then Maxwell's equations for the envelop function lead to a coupled ENLSE. After choosing a polarization and re-scaling the problem, while neglecting effects such as optical self-steepening, higher order dispersion and the delayed Raman response, one finds that the envelop equation can be written as

$$\mathrm{i}\frac{\partial\psi}{\partial z}+\nabla_\perp^2\psi+|\psi|^2\psi=\delta\frac{\partial^2}{\partial t^2}\psi+\rho\psi-\mathrm{i}\nu|\psi|^{2K-1}\psi. \tag{3}$$

Here, ρ is proportional to the Drude electron charge density and t is the retarded time (coordinate time minus the time to propagate from 0 to z at a speed given by the group velocity evaluated at ω_0); see, for example, [10] for a clear discussion of the parameter definitions that arise in non-dimensionalizing this problem.

In this paper we describe a new fourth-order Fourier split-step method for computing time-periodic soliton-like numerical solutions to extended nonlinear Schrödinger type equations that possess azimuthal symmetry. We call this method the Fourier–Bessel algorithm because of the appearance of the *associated Bessel functions* [19] in certain modules of the algorithm. Extensive error analysis is outside the main scope of this paper. However, we have performed an extensive analysis of the evolution of the relative error as the algorithm parameters are varied.

To illustrate the use of this technique, the Fourier–Bessel method is applied to simulate numerical solutions of the ENLSE in a model system that describes the dynamical evolution of a periodic flux of brief (femtosecond) laser pulses that propagate through a nonlinear medium. These numerical experiments exhibit the nonlinear wave propagation as pulse filamentation into soliton-like (quasi-normal) modes, which that each possess a characteristic propagation speed in the medium. Hence the modes may be resolved in time by a family of planes (z-slices) that are transverse to the general propagation direction. Within a slice, each distinct mode appears offset from the time origin (defined as the coordinate time when the space-time center of a chosen initial Gaussian pulse is at the spatial origin of the sample) by a time delay that is inversely proportional to the mode's propagation speed.

We should emphasize the term "exhibit" in the previous paragraph. Our numerical experiments certainly do not prove that the initial Gaussian pulse may be realized as a nonlinear superposition of conjectured (quasi-normal) modes of the ENLSE. Our results are merely consistent with such a picture.

2. Problem definition and evolution equation

Let $\mathbb{E}_3$ denote Euclidean 3-space and $(x,y,z,t)^{\mathrm{T}}\in\mathbb{M}_4$ denote the Cartesian coordinates of a point in Minkowski spacetime $\mathbb{M}_4=\mathbb{E}_3\times\mathbb{R}$. We introduce cylindrical coordinates (r,θ,z) on $\mathbb{E}_3$ such that $x=r\cos(\theta)$ and

$y = r\sin(\theta)$. We restrict our attention to problems possessing azimuthal symmetry so that $\psi = \psi(r, z, t)$. The action of the Laplacian on ψ is $\nabla^2\psi = \left[\frac{\partial^2}{\partial r^2} + \frac{1}{r}\frac{\partial}{\partial r} + \frac{\partial^2}{\partial z^2}\right]\psi = \nabla_\perp^2(r)\psi + \frac{\partial^2}{\partial z^2}\psi$, where $\nabla_\perp^2(r) = \frac{1}{r}\frac{\partial}{\partial r}r\frac{\partial}{\partial r}$.

The problem that we study in order to illustrate the Fourier–Bessel algorithm is the numerical solution of the ENLSE corresponding to the dynamical evolution of a periodic (temporal period $= \tau$) train of brief (femtosecond) Gaussian laser pulses that are incident from vacuum ($z < 0$) on a nonlinear medium that fills the half-space $z \geqslant 0 \in \mathbb{E}_3$. The incident laser pulses possess azimuthal symmetry and initially propagate parallel to the z-axis from vacuum into the nonlinear medium.

The implementation of this numerical algorithm begins with the truncation of the natural infinite intervals corresponding to the coordinate axes of $\mathbb{M}_4$ to finite intervals. The finite interval lengths are chosen to be sufficiently large so that boundary effects do not affect the numerical propagation of solitary waves in the cylindrical region of $\mathbb{E}_3$ for the time interval $\mathcal{T}$ chosen for study. This cylindrical region of $\mathbb{E}_3$ begins at the vacuum-nonlinear medium interface at $z = 0$ and extends into the medium a distance Z. For the numerical experiments considered here we implement the algorithm on the closed point-set $\Omega = \mathcal{C}(R, L_{0,Z}) \times [0, \mathcal{T}]$. Here, $L_{0,\,Z}$ denotes the line segment from point $(0,0,0)^{\mathrm{T}} \in \mathbb{E}_3$ to point $(0,0,Z)^{\mathrm{T}} \in \mathbb{E}_3$ and $\mathcal{C}(R, L_{0,Z})$ denotes the right circular cylinder of radius R and with axis $L_{0,Z}$. In addition we denote the "illuminated" end-cap at $z = 0$ of $\mathcal{C}(R, L_{0,Z}) \times [0, \mathcal{T}]$ by $\partial\Omega = \Omega|_{z=0}$.

The problem that we study here is the numerical solution of

$$\begin{aligned}
&\frac{\partial}{\partial z}\psi = \frac{i}{2k_z}\nabla_\perp^2\psi + i\gamma|\psi|^2\psi - \frac{i}{2!}\beta_2\frac{\partial^2}{\partial t^2}\psi + \frac{1}{3!}\beta_3\frac{\partial^3}{\partial t^3}\psi \quad \text{in } \Omega,\\
&\psi(r, z, t) = \psi(r, z, t + \tau),\\
&\psi(r, 0, t) = f(r, t) \quad \text{on } \partial\Omega.
\end{aligned} \tag{4}$$

The method of solution that we shall discuss may easily be generalized to handle the inclusion of other nonlinear terms $F(\psi^*, \psi)$ (such as $i\nu|\psi|^{2K-1}\psi$) to the ENLSE, providing that the added terms preserve Eq. (7) (below). Here, τ denotes the temporal period and k_z, γ, β_2 and β_3 are given constants. In addition to the last two equations of Eq. (4) we impose two other boundary conditions on $\psi(r, z, t)$, which are listed in Eq. (9) below, that insure that $\int_0^\tau \mathrm{d}t \int_0^\infty r\,\mathrm{d}r|\psi(r, z, t)|^2$ is a constant independent of z.

In this paper we assume that the incident laser pulses are initially Gaussian

$$\begin{aligned}
&f(r, t) = \psi(r, z = 0, t) = \sum_{n=-\infty}^{\infty} f_0(r, t - n\tau),\\
&f_0(r, t) = \sqrt{\frac{2P_{\mathrm{in}}}{\pi w_0^2}}\mathrm{e}^{-\left\{\frac{r}{w_0}\right\}^2}\mathrm{e}^{-\left\{\frac{t}{t_{\mathrm{p}}}\right\}^2}\mathrm{e}^{-\mathrm{i}\frac{k_z}{2F_{\mathrm{L}}}r^2},
\end{aligned} \tag{5}$$

where P_{in}, w_0, t_{p}, andF_{L} denote the input peak power, waist, duration, and focal length, respectively. In the model calculations for this paper the values of P_{in} and t_{p}, respectively, are chosen to be just below (respectively, above) the numerically determined thresholds for beam collapse; similarly for w_0 and F_{L}. It is in this parameter regime where one might expect to see the greatest dependence of the algorithm on its parameters N_r, N_z and N_t, which are defined below. In these numerical experiments we always use the parameter values $P_{\mathrm{in}} = \pi, w_0 = \frac{1}{\sqrt{2}}, t_{\mathrm{p}} = \frac{1}{200\sqrt{ln(2)}}$, and $F_{\mathrm{L}} \to \infty$.

Eq. (4) implies that the modulus-squared of ψ changes with z according to

$$\begin{aligned}
\frac{\partial}{\partial z}|\psi|^2 = {}& \frac{1}{r}\frac{\partial}{\partial r}\left\{\frac{\mathrm{i}}{2k_z}\left[r\left(\psi^*\frac{\partial\psi}{\partial r} - \psi\frac{\partial\psi^*}{\partial r}\right)\right]\right\}\\
&+ \frac{\partial}{\partial t}\left\{-\frac{\mathrm{i}\beta_2}{2!}\left[\psi^*\frac{\partial\psi}{\partial t} - \psi\frac{\partial\psi^*}{\partial t}\right] + \frac{1}{3!}\beta_3\left[\frac{\partial^2}{\partial t^2}|\psi|^2 - 3\left|\frac{\partial\psi}{\partial t}\right|^2\right]\right\}.
\end{aligned} \tag{6}$$

Integration over a temporal period τ and from $0 \leqslant r < \infty$ while invoking appropriate boundary conditions on the "fluxes" that appear in this equation lead to the important conclusion that

$$\frac{\partial}{\partial z}\int_0^\tau \mathrm{d}t \int_0^\infty 2\pi r\,\mathrm{d}r|\psi(r,z,t)|^2 = 0. \tag{7}$$

In this paper we restrict our attention to problems that satisfy boundary conditions such that

$$L_2[\psi](z) \equiv \int_0^\tau \mathrm{d}t \int_0^\infty 2\pi r\,\mathrm{d}r|\psi(r,z,t)|^2 \tag{8}$$

is a constant independent of z, namely, Inspection of Eq. (6) gives sufficient conditions for this as

$$\begin{aligned}
&\lim_{r\to 0}\left\{r\left(\psi^*\frac{\partial\psi}{\partial r} - \psi\frac{\partial\psi^*}{\partial r}\right)\right\} = \lim_{r\to\infty}\left\{r\left(\psi^*\frac{\partial\psi}{\partial r} - \psi\frac{\partial\psi^*}{\partial r}\right)\right\}\\
&\lim_{t\to 0^+}\left\{-\frac{\mathrm{i}\beta_2}{2!}\left[\psi^*\frac{\partial\psi}{\partial t} - \psi\frac{\partial\psi^*}{\partial t}\right] + \frac{1}{3!}\beta_3\left[\frac{\partial^2}{\partial t^2}|\psi|^2 - 3\left|\frac{\partial\psi}{\partial t}\right|^2\right]\right\}\\
&\quad = \lim_{t\to\tau^-}\left\{-\frac{\mathrm{i}\beta_2}{2!}\left[\psi^*\frac{\partial\psi}{\partial t} - \psi\frac{\partial\psi^*}{\partial t}\right] + \frac{1}{3!}\beta_3\left[\frac{\partial^2}{\partial t^2}|\psi|^2 - 3\left|\frac{\partial\psi}{\partial t}\right|^2\right]\right\}.
\end{aligned} \tag{9}$$

The definition of the Fourier–Bessel algorithm proceeds as follows: Formal integration of the first equation in Eq. (4) yields the approximation,

$$\psi(r,z+\Delta z,t) = \exp\{\Delta z(A+B+C)\}\psi(r,z,t), \tag{10}$$

where

$$A = -\frac{\mathrm{i}}{2!}\beta_2\frac{\partial^2}{\partial t^2} + \frac{1}{3!}\beta_3\frac{\partial^3}{\partial t^3}, \tag{11}$$

$$B = \mathrm{i}\gamma|\psi|^2 \tag{12}$$

and

$$C = \frac{\mathrm{i}}{2k_z}\nabla_\perp^2. \tag{13}$$

To approximate the action of the exponential operator in Eq. (10) we employ an obvious generalization of a fourth-order symmetrized approximant of $\exp[\Delta z(A+B)]$ that has been advocated by Hatano and Suzuki [20,21]. Let

$$S_2(\Delta z) \equiv \exp\left(\frac{\Delta z}{2}A\right)\exp\left(\frac{\Delta z}{2}B\right)\exp(\Delta z C)\exp\left(\frac{\Delta z}{2}B\right)\exp\left(\frac{\Delta z}{2}A\right) \tag{14}$$

and construct a symmetrized fourth-order approximant from this symmetrized second-order approximant according to

$$S_4(\Delta z) \equiv S_2(s_2\Delta z)^2 S_2((1-4s_2)\Delta z)S_2(s_2\Delta z)^2, \tag{15}$$

where $\frac{1}{s_2} = 4 - 4^{1/3}$. Hatano and Suzuki choose the arguments of S_j, $j = 2,4$ so that [1] the first-order term in the Taylor series expansion of S_j is $\Delta z(A+B+C)$; and [2] the whole product S_j is symmetrized, and satisfies $S_j(\Delta z)S_j(-\Delta z) = \mathbb{I}$.

Hatano and Suzuki [20] point out that the simpler symmetrized fourth-order approximant [22]

$$S_4'(\Delta z) \equiv S_2(s_1\Delta z)S_2((1-2s_1)\Delta z)S_2(s_1\Delta z), \tag{16}$$

where $\frac{1}{s_1} = 2 - 2^{1/3}$, will in general propagate ψ to 'times' earlier than those specified by the initial data. As is evident, the product equation (16) has a part that goes into the past (in this case, $z < 0$). This can be problematic in systems without time-reversal symmetry such as diffusion from an initial delta-functional, for example.

In such a case there exists no past given the initial delta distribution. The product equation (15) does not have this possible problem and hence is adopted here.

The numerical approximation of the solution to Eq. (4) is henceforth formulated on a finite discrete lattice embedded in a $3+1$-dimensional $\mathbb{M}_4$. We employ uniform discrete lattice approximations $t \to t_{n_t} = n_t \Delta t$, $0 \leqslant n_t < N_t \in \mathbb{N}$, $z \to z_{n_z} = n_z \Delta z, 0 \leqslant n_z < N_z \in \mathbb{N}$ with lattice spacings Δt and Δz, respectively. For the radial coordinate $r \to r_{n_r} = \left(n_r + \frac{1}{2}\right)\Delta r, 0 \leqslant n_r < N_r \in \mathbb{N}$. The approximate solution Ψ_{n_r,n_z,n_t} to Eq. (4) is defined as $\psi(r,z,t) \to \psi\left(\left(n_r+\frac{1}{2}\right)\Delta r, n_z\Delta z, n_t\Delta t\right) \equiv \Psi_{n_r,n_z,n_t}$. With this choice for the ranges of (n_r, n_z, n_t) the matrix Ψ_{n_r,n_z,n_t} has $N_r \times N_z \times N_t$ complex components. Formally, temporal periodicity allows one to define $\Psi_{n_r,n_z,n_t'}$ for any positive integer n_t' according to $\Psi_{n_r,n_z,n_t'} = \Psi_{n_r,n_z,n_t}$, where n_t is the remainder after numerical division of n_t' by N_t. In this paper we do not augment Ψ_{n_r,n_z,n_t} with the $N_r \times N_z$ complex components Ψ_{n_r,n_z,N_t} (which would make periodicity explicit through $\Psi_{n_r,n_z,N_t} = \Psi_{n_r,n_z,0}$) because the fast Fourier transform library that we use in implementing this algorithm (FFTW [23]) does not use Ψ_{n_r,n_z,N_t}.

In passing we remark that while the computational overhead of this algorithm is not trivial, it may be efficiently implemented using only desktop hardware. When implemented in Fortran 90 [Intel compiler and Math Kernel Library] on an Intel Core-2 dual-core x6800 platform, and for choices $0 \leqslant r,\ t \leqslant 1$, $\beta_2 = 0, k_z = \frac{1}{2}, \tau = 1 = \gamma = \beta_3$, $\Delta t = \frac{1}{4096}$, $\Delta r = \frac{1}{32}$ and $\Delta z = 0.009$ the (iterative) algorithm executed 3000 z-steps in under 180 min, converging to a fractional change in $L_2[\psi](z)$ of $O(\Delta z^7)$. In another run with $\beta_2 = 1$ and the other parameters unchanged, the program executed in under 180 minutes, $L_2[\psi](z)$ converging to a consistent value within the expected relative tolerance of $O(\Delta z^5)$.

2.1. Numerical algorithm

We shall construct this algorithm from unitary constituents $\exp(xA)$ and $\exp(x\ B)$, $x = \Delta z, \frac{1}{2}\Delta z, \frac{1}{2}(1-4s_2)\Delta z, \ldots$. We shall also represent $\exp(xC)$ such that in the limit $N_r \to \infty$ the action of $\exp(xC)$ is equivalent to a unitary matrix transformation [19]. In this limit, the Fourier–Bessel algorithm is equivalent to a unitary algorithm. For this problem we show that it is possible to truncate N_r to a finite value while preserving the unitarity of the algorithm. Hence the Fourier–Bessel method is unitary, and thus unconditionally stable.

2.1.1. Action of $\exp(xA)$

The action of $\exp(xA)$ on the τ-periodic ψ is implemented using a standard Fourier transform method. Symbolically, $\exp(xA)\psi(\cdot,t) = \mathcal{F}^{-1}[\exp(x\mathcal{F}A\mathcal{F}^{-1})\mathcal{F}[\psi(\cdot,t)]]$, where $\mathcal{F}$ denotes the appropriate Fourier transform. $(\mathcal{F}A\mathcal{F}^{-1})[\omega]$ is conventionally computed in the continuum limit, and then projected onto a finite sequence. We choose an upper bound N_t such that $0 \leqslant n_t < N_t$, and define N_t angular frequencies $\omega_{n_t} = \frac{2\pi}{N_t} n_t$. Both the indexing and the range for ω are chosen to be consistent with the discrete Fourier transform library (FFTW [23]) that we use. $(\mathcal{F}A\mathcal{F}^{-1})[\omega]$ is evaluated at these frequencies. The operator $(\mathcal{F}A\mathcal{F}^{-1})[\omega]$ is diagonal in frequency space, with diagonal element D_{n_t,n_t} equal to a polynomial in ω_{n_t}. Next the discrete Fourier transform corresponding to $\mathcal{F}[\psi(\cdot,t)] \to \tilde{\psi}(\cdot,\omega)$ is computed. The computation of the action $\exp(xA)$ on ψ is completed by computing the discrete inverse transform of the product sequence $\exp[x'(\mathcal{F}A\mathcal{F}^{-1})[\omega]]_{n_t,n_t}\widetilde{\Psi}(\cdot,\omega)_{n_t}$.

2.1.2. Action of $\exp(xC)$

The action of $\exp(xC)$ on ψ is implemented as follows: For problems possessing azimuthal symmetry $\psi(r,\theta,z,t) = \psi(r,z,t)$ and the action of the Laplacian on ψ is $\nabla^2\psi = \left[\frac{\partial^2}{\partial r^2} + \frac{1}{r}\frac{\partial}{\partial r} + \frac{\partial^2}{\partial z^2}\right]\psi = \left[\nabla_\perp^2(r) + \frac{\partial^2}{\partial z^2}\right]\psi$, where $\triangle_\perp(r) \equiv \nabla_\perp^2 = \frac{1}{r}\frac{\partial}{\partial r} r \frac{\partial}{\partial r}$. The action of $\triangle_\perp(r)$ on ψ is approximated (suppressing n_z and n_t) by $\{\triangle_\perp(r)\Psi\}_{n_r} \approx \frac{1}{\Delta r^2}(\mathbb{T}\Psi)_{n_r}$, where $(\mathbb{T}\Psi)_{n_r} = \Psi_{n_r+1} - 2\Psi_{n_r} + \Psi_{n_r-1} + \frac{1}{2\left(n_r+\frac{1}{2}\right)}(\Psi_{n_r+1} - \Psi_{n_r-1})$. The matrix elements of $\mathbb{T}$ are

$$\mathbb{T}_{nn'} = \delta_{nn'-1}\left(1 + \frac{1}{2\left(n+\frac{1}{2}\right)}\right) + \delta_{nn'}(-2) + \delta_{nn'+1}\left(1 - \frac{1}{2\left(n+\frac{1}{2}\right)}\right), \tag{17}$$

where $n, n\prime \in \mathbb{N}$. It is known [19] that the matrix

$$\mathbb{S} \equiv \mathrm{e}^{\frac{\mathrm{i}}{2}\lambda\mathbb{T}}, \tag{18}$$

with $\lambda = \frac{1}{k_z}\frac{\Delta z}{\Delta r^2}$, is similar to a unitary matrix $\mathbb{U}$ times a phase factor:

$$\mathbb{S} = \mathrm{e}^{-\mathrm{i}\lambda}\mathbb{W}^{-1}\mathbb{U}\mathbb{W}, \tag{19}$$

where the "weight" matrix $\mathbb{W}$ has matrix elements

$$\mathbb{W}_{nn'} = \delta_{nn'}\sqrt{2n+1}, \tag{20}$$

$n, n' \in \mathbb{N}$; $\mathbb{W}^\dagger\mathbb{W}$ corresponds to the radial weight function r in this cylindrical coordinate system. The matrix elements of $\mathbb{U}$ are given by the associated Bessel functions [19]

$$\mathbb{U}_{nn'}(\lambda) = \frac{1}{2}\sqrt{\frac{(1+2n)(1+2n')}{2\pi\lambda}}\sum_{k=|n-n'|,\ k\to k+2}^{n+n'} i^k(1+2k)\gamma_{nn'k}J_{k+\frac{1}{2}}(\lambda), \tag{21}$$

where

$$\gamma(k) \equiv \frac{\Gamma\left(\frac{1}{2}(1+k)\right)}{\Gamma\left(\frac{1}{2}(2+k)\right))} \tag{22}$$

and

$$\gamma_{nn'k} \equiv \gamma(1+n+n'+k)\gamma(-n+n'+k)\gamma(n-n'+k)\gamma(n+n'-k). \tag{23}$$

Here, $J_\nu(\lambda)$ denotes the order ν Bessel function of the first kind.

The Fourier–Bessel algorithm employs the operator approximation,

$$\exp(xC) = \mathrm{e}^{-\mathrm{i}x\lambda}\mathbb{W}^{-1}\mathbb{U}(x\lambda)\mathbb{W}. \tag{24}$$

We have restricted the problem to a finite region of the r-axis by selecting an upper bound N_r such that $0 \leqslant n_r < N_r$. Of course the truncated $N_r \times N_r$ matrix $\mathbb{U}$ is no longer exactly unitary. However, in virtue of Eq. (7), we may restore unitarity simply by renormalizing Ψ at the end of each z-step.

If one examines the asymptotic expansion of $J_\nu(\lambda)$ then one sees that it decreases exponentially for large $\frac{\nu}{\lambda}$. Unless there is an application-related reason to modify λ during the computation, the two Bessel function sequences that appear in the algorithm once Eq. (15) is expanded, namely, $J_\nu(\lambda)$ and $J_\nu\left(\lambda\left(4-\frac{1}{s_2}\right)\right)$, are ordinarily calculated only once, at the beginning of the computation. The value of λ is chosen so that the last retained $J_{2N_r+\frac{1}{2}}(\lambda)$ and $J_{2N_r+\frac{1}{2}}\left(\lambda\left(4-\frac{1}{s_2}\right)\right)$ are both much less in magnitude than $\mathrm{O}(\Delta z^5)$. In this paper we use a fixed value of $\lambda = 7.72525$, which satisfies this criterion, for all runs of the Fourier–Bessel method so that the algorithm dependence on N_r and N_t can be studied.

2.1.3. Action of exp(x B) and iterative algorithm

Assume that we know $\psi(r, z=0, t)$ from initial data, and have evolved forward using Eq. (10) in z-space so that $\psi(r, z=n_z\Delta z, t)$ is also known $\forall r = \left(n_r+\frac{1}{2}\right)\Delta r, t = n_t\Delta t$. We now define a process for stepping from z to $z+\Delta z$ that is governed by $\exp\{\Delta z(B)\}$. There are two common ways to treat the "lumped" nonlinearity contained in a symmetrized approximant of $\exp\{\Delta z(A+B+C)\}$. The conventional split-step method may be symbolically formulated as $\psi\left(r, z+\frac{1}{2}\Delta z^+, t\right) = \exp\{\Delta z(B)\}\psi\left(r, z+\frac{1}{2}\Delta z^-, t\right)$. It is well known that this method is accurate to $\mathrm{O}(\Delta z^2)$. However the symmetrized split-step iterative method, an example of which is defined below, is accurate to $\mathrm{O}(\Delta z^3)$. We adopt a symmetrized split-step iterative method.

To begin the process of stepping from z to $z+\Delta z$ we define three $N_t \times N_r$ complex arrays u_0, u_1, and u_{01}, and initialize u_0 and u_1 according to $u^{n_t}_{0n_r} = u^{n_t}_{1n_r} = \psi\left(\left(n_r+\frac{1}{2}\right)\Delta r, z, n_t\Delta t\right) = \Psi_{n_r,n_z,n_t}$. Introducing a mixing parameter mix, $\frac{1}{2} < \mathrm{mix} < 1$, we set $u_{01} = \mathrm{mix}u_0 + (1-\mathrm{mix})u_1$ and compute

$$B = \mathrm{i}\gamma|u_{01}|^2. \tag{25}$$

u_1 is updated using $u_1 = \psi(r, z+\Delta z, t) = \exp\{\Delta z(A+B+C)\}u_{01}$, where it is understood that the symmetrized fourth-order approximant defined in Eq. (15) replaces $\exp\{\Delta z(A+B+C)\}$. This process is iterated by resetting $u_{01} = \mathrm{mix}u_0 + (1-\mathrm{mix})u_1$, computing $B = \Delta z i\gamma|u_{01}|^2$, and then again updating u_1 using

$$u_1 = \exp\{\Delta z(A + B + C)\}u_{01}, \tag{26}$$

until the fractional change in the discrete version of $L_2[\psi](z), \sum_{n_t,n_r} \Delta t\left[2\pi\left(n_r + \frac{1}{2}\right)\Delta r\right]|u_1|^2_{n_r,n_z,n_t}$, is $O(\Delta z^5)$ or less. For the numerical experiments conducted in this paper the number of iterations required for convergence always fewer than 10, and was never too sensitive to the particular value of the mixing parameter. The optimal value of the mixing parameter depends both on the parameters in the partial differential equation and on the other algorithm parameters, but no analytic formula that might be used to calculate it is known. The fixed $\text{mix} = \frac{3}{4}$ was used in all of the calculations below.

3. Discussion

3.1. Stability of the Fourier–Bessel algorithm

First let us briefly recall a few definitions and conventions. In this paper $t \to t_{n_t} = n_t\Delta t, 0 \leqslant n_t < N_t \in \mathbb{N}$, $r \to r_{n_r} = \left(n_r + \frac{1}{2}\right)\Delta r, 0 \leqslant n_r < N_r \in \mathbb{N}$ and $z \to z_{n_z} = n_z\Delta z, 0 \leqslant n_z < N_z \in \mathbb{N}$ with lattice spacings $\Delta t = \frac{1}{N_t}$, $\Delta r = \frac{1}{N_r}$ and $\Delta z = \lambda k_z \Delta r^2$, respectively. The numerical approximation Ψ_{n_r,n_z,n_t} of the solution to Eq. (4) is defined by $\Psi_{n_r,n_z,n_t} \equiv \psi\left(\left(n_r + \frac{1}{2}\right)\Delta r, n_z\Delta z, n_t\Delta t\right)$. The relative intensity at a grid node $\mathcal{I}^{N_t}_{n_r,n_z,n_t} = |\Psi_{n_r,n_z,n_t}|^2$ is used to title Figs. 1–3. This notation makes explicit the length N_t of the discrete Fourier transform used in computing Ψ_{n_r,n_z,n_t}. For brevity, $\mathcal{I}_{N_t}$ is used for $\mathcal{I}^{N_t}_{n_r,n_z,n_t}$ in discussion and in captioning for the figures in this paper.

We have constructed the Fourier–Bessel algorithm from unitary realizations of the operators $\exp(xA)$ and $\exp(xB)$. After restoring unitarity at each z-step by renormalizing Ψ, the renormalized operator associated to $\exp(xC)$ is also unitary. Hence this algorithm is unitary and therefore unconditionally stable.

The questions of absolute error and global accuracy of this method as a function of the lattice spacings Δr, Δz and Δt, or equivalently, the parameters N_r, N_z, and N_t, are important but not directly studied in this paper. Estimating the absolute accuracy of algorithms that provide numerical solutions to nonlinear problems is

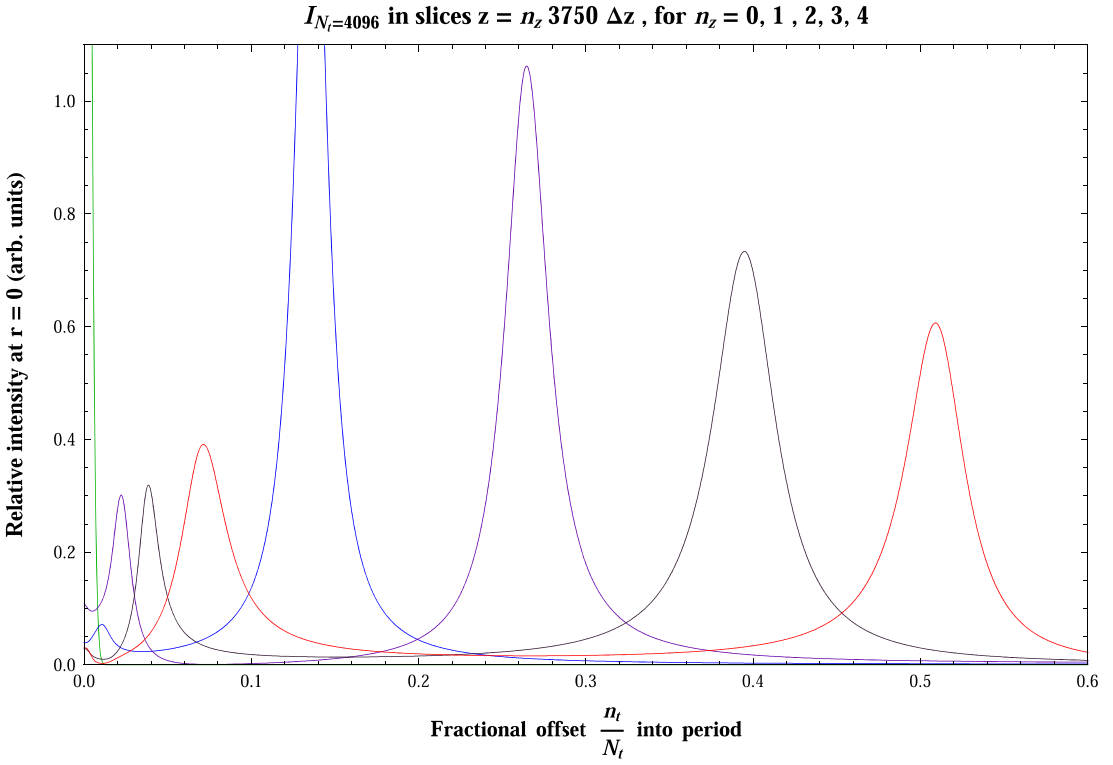

Fig. 1. Resolution of quasi-normal modes of characteristic propagation speed; the incident Gaussian pulse at $z = 0$ is centered about $\frac{n_t}{N_t} = 0$.

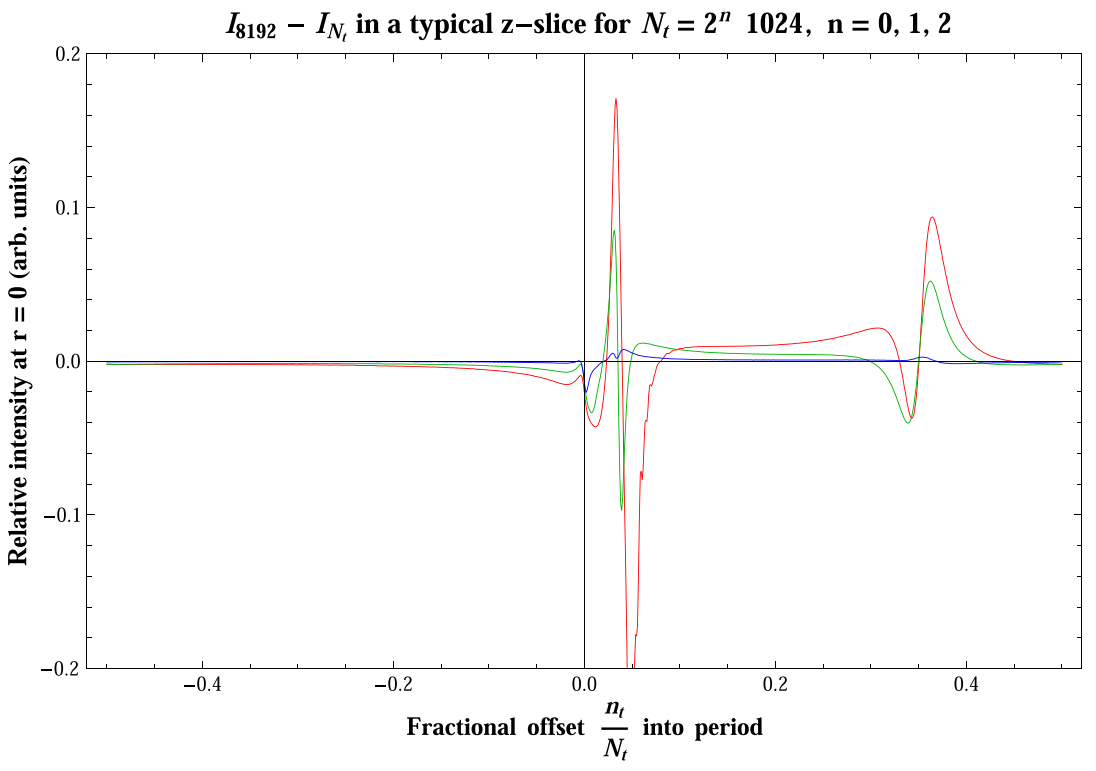

Fig. 2. Convergence to a common temporal history with increasing N_t.

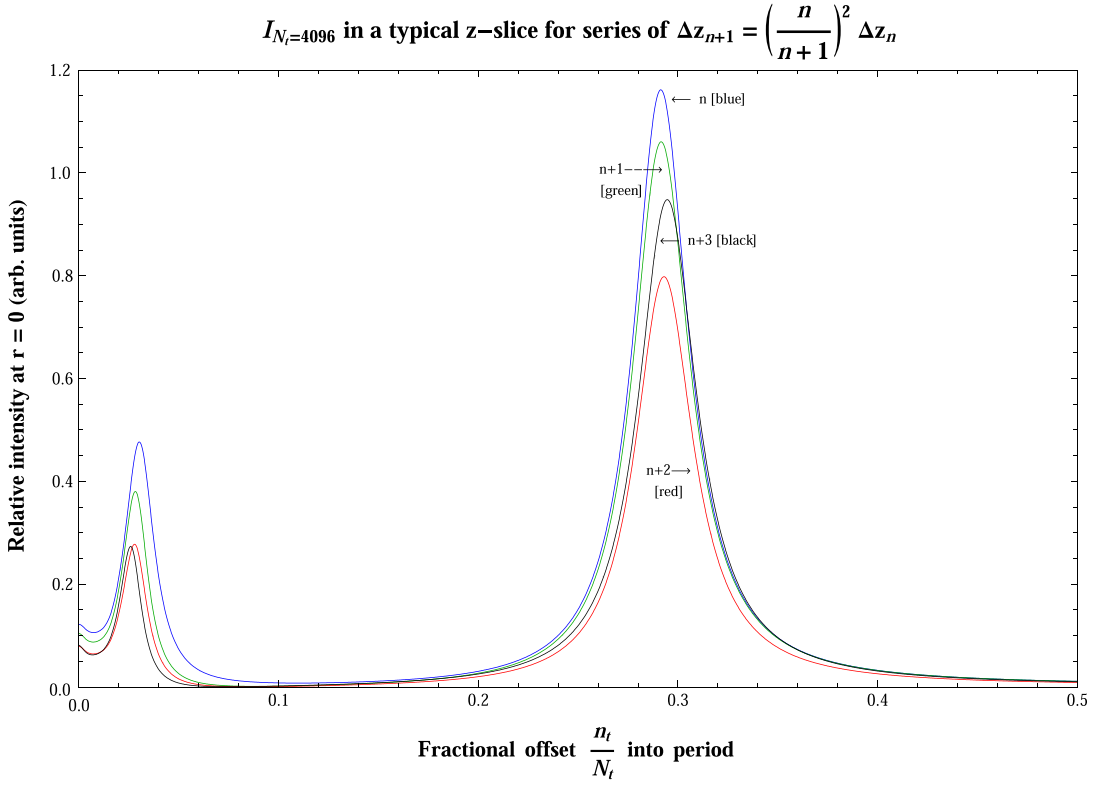

Fig. 3. Convergence to a common temporal history with decreasing Δz.

problematic for cases in which exact analytic solutions are not known, and especially when these problems possess few known conserved quantities. The question of absolute accuracy of this algorithm must be deferred. Instead we document the typical approach to a converged value for Ψ_{n_r,n_z,n_t} at each node of our grid as a function of algorithm parameters, but unfortunately we are unable to comment on the absolute accuracy of the converged value. In applications of this algorithm the measure of accuracy and error may be empirical, and ultimately rest upon the answer to the old question, "does theory correctly predict what is measured?"

3.2. Numerical experiments

With this in mind let us now employ the Fourier–Bessel algorithm to predict the characteristics of the propagation through a nonlinear medium of a periodic series of short laser pulses. Using the ENLSE we model the propagation of the normally incident flux of Gaussian pulses given by Eq. (5) as they propagate from vacuum into a homogeneous medium that occupies the region of $\mathbb{M}_4$ given by $z > 0$. As mentioned above, the boundary between vacuum and the homogeneous medium is the $z = 0$ plane. The optic axis is the z-axis, and the pulses generally propagate parallel to this axis. The phrase 'z-slice' is used to refer to the transverse plane that passes through z and is parallel to the xy-plane. We show that, as the wave propagates through the medium, soliton-like normal modes in the waveform intensity may be resolved in time by a family of z-slices that spatially resolve the z-axis (please refer to Fig. 1). We refer to this space-time resolution of modes as 'normal mode condensation'. It is a manifestation of pulse filamentation. Experimentally, pulse filamentation due to various effects is a well-known phenomenon.

Soliton (quasi-)normal modes may be identified by plotting the waveform intensity over a portion of one temporal period in a z-slice. For the sake of simplicity, only the intensity at $r = 0$ is displayed in the figures. The graphs in Fig. 1 record the on-axis waveform intensities (arbitrary units) of five particular z-slices over a common part of a temporal period The incident Gaussian pulse in slice $z = 0$ is centered about $\frac{n_t}{N_t} = 0$ in this figure. The graphs in Fig. 1 reveal two modes, the slower of the two initially possessing most of the power. As the laser pulse propagates downstream (toward increasing z) these modes tend to distribute the power more evenly. Parameter values for these runs were $N_r = 44$, $N_t = 4096$, $\Delta r = \frac{1}{N_r}$, $\Delta t = \frac{1}{N_t}$, $k_z = \frac{1}{2}$ and $\tau = 1 = \gamma = \beta_2 = \beta_3$.

Next the dependence of the convergence of $\mathcal{I}_{N_t}$ as a function of N_t is studied. Except for allowing $N_t = 2^n \times 1024$, $n = 0, 1, 2, 3$ to vary, we use the same parameter values as before. Fig. 2 exhibits the typical convergence to a common temporal history as a function of increasing N_t. This behavior was seen in all numerical trials. Generally for fixed $\frac{n_t}{N_t}$, the change in a value of $|\mathcal{I}_{N_t=8192} - \mathcal{I}_{N_t}|$ from one trial to the next monotonically decreased as N_t was increased.

Lastly the dependence of the convergence of $\mathcal{I}_{N_t}$ as a function of N_r is studied. A sequence $\Delta z_{n+1} = \left(\frac{n}{n+1}\right)^2 \Delta z_n$ is defined by increasing N_r in the relationship $\Delta z = \lambda \Delta r^2 k_z$. Here, $N_t = 4096$, but other than N_r we use the same parameter values as before. Fig. 3 displays a representative instance of a Δz_n series. Pictured are four trials, starting with $n = 41$. For each fixed $\frac{n_t}{N_t}$ value the sequence of intensity values suggests that after some positive integer n_{Z_0}, the sequence of differences in $\mathcal{I}_{N_t}$ from a conjectured limit may be Cauchy.

4. Conclusion

Pulse filamentation in a familiar phenomenon. The Fourier–Bessel method has been shown to be capable of at least qualitatively resolving pulse filamentation. The Fourier–Bessel method may prove to be powerful enough to be adapted to provide numerical solutions of pulse propagation problems for other systems that are governed by linear and nonlinear, local and non-local, Schrödinger type equations. These effects may have important implications and applications in practical fields such as laser-initiated fusion and optical communications.

References

[1] F.D. Tappert, Numerical solutions of the Korteweg de Vries equation and its generalizations by the split-step Fourier method (cited in [2]).
[2] F.D. Tappert, C.N. Judice, Recurrence of nonlinear ion acoustic waves, Phys. Rev. Lett. 29 (1972) 1308–1311.

[3] M.D. Feit, J.A. Fleck Jr., A. Steiger, Solution of the Schrödinger equation by a spectral method, J. Comput. Phys. 47 (1982) 412.
[4] Y.S. Kivshar, B.A. Malomed, Solitons in nearly integrable systems, Rev. Mod. Phys. 61 (1989) 763–915.
[5] G.P. Agrawal, Nonlinear Fibre Optics, Academic Press, NY, 1989.
[6] M. Gedalin, T.C. Scott, Y.B. Band, Phys. Rev. Lett. 78 (1997) 448.
[7] G. Fibich, G. Papanicolao, Self-focusing in the perturbed and unperturbed nonlinear Schrodinger equation in critical dimension, SIAM J. Appl. Math. 60 (1999) 183–240.
[8] P. Sprangle, J.R. Penano, B. Hafizi, Propagation of intense short laser pulses in the atmosphere, Phys. Rev. E 66 (2002) 046418.
[9] L. Bergé, S. Skupin, Phys. Rev. E 71 (2005) 065601(R).
[10] S. Skupin, R. Nuter, L. Bergé, Optical femtosecond filaments in condensed media, Phys. Rev. A 74 (2006) 043813.
[11] S. Skupin, L. Bergé, Physica D 220 (2006) 14.
[12] S. Eisenmann, A. Pukhov, A. Zigler, Fine structure of a laser-plasma filament in air, Phys. Rev. Lett 98 (2007) 155002.
[13] D.L. Feder, C.W. Clark, B.I. Schneider, Nucleation of vortex arrays in rotating anisotropic Bose–Einstein condensates, Phys. Rev. A 61 (1999) 011601.
[14] J.R. Abo-Shaeer, C. Raman, J.M. Vogels, W. Ketterle, Observation of vortex lattices in Bose–Einstein condensates, Science 292 (2001) 476.
[15] A. Aftalion, Q. Du, Vortices in a rotating Bose–Einstein condensate: critical angular velocities and energy diagrams in the Thomas–Fermi regime, Phys. Rev. A 64 (2001) 063603.
[16] S.K. Adhikari, P. Muruganandam, Effect of an impulsive force on vortices in a rotating Bose–Einstein condensate, Phys. Lett. A 301 (2002) 333–339.
[17] W. Bao, Ground states and dynamics of multi-component Bose–Einstein condensates, Multiscale Model. Simulat. 2 (2004) 210–236.
[18] W. Bao, Q. Du, Y. Zhang, Dynamics of rotating Bose–Einstein condensates and their efficient and accurate numerical computation, SIAM J. Appl. Math., in press.
[19] P.L. Nash, R. López-Mobilia, Associated Bessel functions and the discrete approximation of the free-particle time evolution operator in cylindrical coordinates, J. Math. Phys. 45 (2004) 1988–1993, doi:10.1063/1.1695601.
[20] N. Hatano, M. Suzuki, Finding exponential product formulas of higher orders, Lect. Notes Phys. 679 (2005) 3768.
[21] M. Suzuki, General theory of higher-order decomposition of exponential operators and symplectic operators, Phys. Lett. A 165 (1992) 387.
[22] G.M. Muslu, H.A. Erbay, Higher-order split-step Fourier schemes for the generalized nonlinear Schrodinger equation, Math. Comp. Simul. 67 (2005) 581595.
[23] Matteo Frigo, Steven G. Johnson, The Design and Implementation of FFTW3, in: Proceedings of the IEEE 93(2) (2005) 216231 [<http://www.fftw.org/>].